INTERNATIONAL JOURNAL OF RESEARCH IN COMPUTER APPLICATIONS AND ROBOTICS
ISSN 2320-7345

NODULE DETECTION IN LUNG INTERVENTION BY USING VDE AND MORPHOLOGY TECHNIQUES

[1]C.M. Niranjana, ME,
Department of Computer Science and Engineering, Muthayammal Engineering College, Rasipuram.
E-mail: niranjana5790@gmail.com

[2]P.Deepa, asst.professor,
Department of Computer Science and Engineering, Muthayammal Engineering College, Rasipuram.
E-mail: Deeparam2000@gmail.com

Abstract

Lung cancer is the serious cause of death, since identification of such nodule at an early stage is difficult task. Thus the CADe scheme is developed for detection of pulmonary nodules by use of the VDE with MTANN techniques and mathematical morphology to improve the sensitivity for nodules overlapping ribs and clavicles and to reduce the False Positives caused by these structures. The Virtual Dual Energy is the image processing technique used to suppress the rib and clavicle. The Massive Training Artificial Neural Network is adequately trained with a small number of cases to demonstrate the distinction between nodules and vessels in thoracic Computed Tomography images. The trained MTANN would be robust against a change in scale and rotation. The stochastic watershed transformation technique is used for segmentation tool whenever the minima of the image represent the objects of interest and the maxima of the image represent the separation boundaries between objects. And to provide experiment results based on MTANN techniques and mathematical morphology with reduction of False positives and to improve more segmentation accuracy.

Keywords: Computed Tomography, False positives, Virtual Dual Energy.

1. INTRODUCTION

1.1 COMPUTER-AIDED DETECTION

Computer-Aided Detection for lung nodules on Chest Radiographs has been investigated for assisting radiologists in improving their sensitivity in the detection of lung nodules. Although a great deal of work has been done by researchers to improve the performance of CADe schemes for nodule detection on CXRs, CADe schemes still produce a relatively large number of False Positives. This would distract radiologists in their detection and reduce radiologist's efficiency.

The radiologists may lose their confidence in the CADe scheme as a useful tool, which may result in less improved performance of radiologists. A major challenge for current CADe schemes for nodule detection on CXRs is to detect the nodules overlapping ribs, rib crossings, and clavicles, because majorities of FPs are caused by these structures. This leads to lowering the sensitivity as well as the

Specificity of a CADe scheme. In order to detect nodules that overlap ribs and clavicles and to reduce the FP rate often caused by ribs and clavicles in standard CXRs, A CADe scheme based on single-exposure dual energy Computed Radiography .

A dual-energy subtraction technique is used for separating soft tissue from bones in CXRs by use of two x-ray exposures at two different energy levels. The dual energy subtraction technique produces soft-tissue images from which bones are extracted. By use of dual-energy soft-tissue images, the performance of their CADe scheme was improved. In spite of its great advantages, only a limited number of hospitals use a dual-energy radiography system, because specialized equipment is required.

The radiation dose can be more than double compared to that for standard CXR. To address the issue of the availability of dual-energy radiography systems, an image-processing technique called Virtual Dual-Energy radiography for suppressing ribs and clavicles in CXRs by means of a multi-resolution MTANN. The real dual-energy images were used as the teaching images for training of the multi-resolution MTANN.

1.2 PULMONARY NODULE DETECTION ON CT

Chest Radiography remains the most commonly ordered radiological examination. Unfortunately, radiography has low sensitivity for demonstrating significant lesions and a high false positive rate for the detection of pulmonary nodules. The greater degree of spatial and contrast resolution provided by Multi-Detector Computed Tomography enables improved sensitivity and specificity for pulmonary nodule detection. However, pulmonary nodules are still undetected on MDCT due to their small size, low Hounsfield unit attenuation, per vascular central orendo bronchial location, or adjacent parenchyma disease.

1.3 MULTI-DETECTOR COMPUTED TOMOGRAPHY

The widespread availability of MDCT scanners provides the opportunity to examine thin-section CT images in the order of 2mm and smaller in thickness, which improves reader detection of focal lung findings and characterization of these findings as nodules. However, the number of images to be examined increases by 5-fold when 1-mm-section images is used instead of 5-mm-section images, which can contribute to reader fatigue. In addition, on thin sections, small pulmonary nodules are difficult to differentiate from normal vascular structures.

Post processing techniques are now widely available and can increase reader sensitivity for pulmonary nodules. The Maximum Intensity Projection technique displays the brightest voxel along an array within a slab. In the lung, the voxels of a vessel are the brightest in contrast to the surrounding air-filled acini, and therefore their values are most often used for display. This leads to visualization of the branching vessel within a slab and facilitates differentiation of a per vascular nodule from the vessel.

The value of MIPs has been shown in both axial and coronal projections, in addition to coronal multilane reformations. Minimum intensity projection images may potentially play a role in the detection of ground-glass lesions image analysis methods can aid the radiologist in detecting lung nodules. These computer algorithms have been enabled by high-resolution thin section MDCT data. CAD techniques have been shown to increase the detection of small pulmonary nodules while maintaining time efficiency for diagnosis.

CAD devices for nodule identification have been primarily investigated in the role of a second reader, in which CAD identifications are viewed subsequent to an initial review by the radiologist. For example a CAD device

increased reader sensitivity for the detection of pulmonary nodules from 50% to 76%, with 3 false-positive detections per CT scan if all the true-positive CAD marks were to be accepted by readers.

False-positive detections by CAD were related to artifact, branching points of vessels, or central vessels, and have been reduced with improved CAD schemes to 3 or fewer per CT scan. The maintenance of a low false-positive rate is important, as radiologist confidence in detecting small pulmonary nodules can be influenced by CAD. A recent study demonstrated that a radiologist will accept 11% of false positive CAD marks. Both CAD and MIP were shown to assist the detection of lung nodules to equal degrees.

The utilization of CAD will be facilitated by seamless viewing of CAD results on clinical Picture Archiving and Communication Systems rather than on a stand-alone workstation, and by ultimately, real-time interaction with CAD. Minimal investigation has been devoted towards CAD identification of ground-glass nodules. CAD detection of ground-glass nodules is difficult. The faint attenuation and low contrast of ground-glass nodules relative to the adjacent lung parenchyma hinder thresholding and segmentation techniques. For example, the sensitivity of a single CAD technique was only 53% for ground-glass nodules, whereas it was 73% for a mixed ground-glass and solid nodule. As this technology continues to evolve, potential exists for devices to positively impact reader detection of lung nodules for both ground-glass and solid attenuation nodules.

Nodule-detection techniques are also needed for automated matching of lung nodules on multiple chest CT studies, an essential aspect of nodule characterization. The process of both nodule detection and image registration requires lung segmentation, feature extraction, and characterization by CAD. The comparison of multiple CT studies poses challenges given variations in aspiratory lung volumes, patient positioning, and lung pathology.

Registration techniques to overcome these challenges include rigid methods that account for patient rotation and location of the patient's thorax within the image, however, differences related to scale and changes in lung, lobe, and loco regional morphology that frequently occur are better addressed with deformable models and elastic registration techniques. Similar methods are used for inter modality registration, such as CT with magnetic resonance imaging. The evaluated study refers a computer registration program's ability to automatically match pulmonary nodules on 3 serial screening MDCTs. They demonstrated 92.7% matching rate between studies performed 1 year apart. Automated matching was not significantly affected by nodule size or ground-glass attenuation.

1.4 NODULE MORPHOLOGY ON MDCT AND ETIOLOGIES

Benign nodules result primarily from infection. Infectious granulomas account for more than 80% of benign SPNs with mycobacterium infection the most common cause, followed by fungal organisms. Hamartomas, consisting of multiple mesenchymal tissue histologies, represent 10% of benign SPNs. Arteriovenous malformations and aneurysms are other causes of an SPN. Malignant etiologies for SPNs include primary lung cancer is 84% and solitary metastasis is 8%. CT trials for lung cancer screening have found an 8% to 51%prevalence of SPNs in high-risk patients.

The most common histological subtype of lung cancer is adeno carcinoma. Adeno carcinoma represents 50% of malignant pulmonary nodules and is typically peripheral in location. Squamous cell carcinoma is the second most common histologic subtype of lung cancer, and two-thirds of these tumors are located centrally. Other subtypes of lung carcinoma can also present as SPNs. Small cell carcinoma occurs as an SPN approximately 5% of the time and more often presents with bulky lymphadenopathy in the hilar and meditational regions.

Carcinoid tumors are neuroendocrine tumors that represent 1% to 2% of all lung tumors, with 10% to 20% atypical and the remainder typical. In addition, 16% to 40% of carcinoids occur in the peripheral lung. Although most often multiple, metastases to the lung parenchyma from an extra pulmonary primary malignancy such as colon and renal cell carcinoma, testicular cancer, melanoma, and sarcoma can appear as SPNs. Lymphoma in the lung parenchyma has several appearances, including that of an SPN.

Size is a primary factor in determining the risk for malignancy of a nodule. In a meta-analysis of 8 large screening trials, the prevalence of malignancy depended on the size of the nodules, ranging from 0% to 1% for nodules 5mm or smaller, 6% to 28% for those between 5 and 10 mm, and 64% to 82% for nodules 20mm or larger.

The presence of multiple nodules increases the likelihood of etiologies such as metastatic disease, septic emboli, and pulmonary infarcts.

2. LUNG CT IMAGE

The lung CT images comprise small noise when compared to scan image and MRI image. The MRI takes more cost, time and provides less details compared to CT image. So we can take the CT images for detecting the lungs. In a CT image, overlapping structures are eliminated, building the internal anatomy more apparent. CT images show the surgeons accurately where to operate. Without this information, the success of surgery is greatly Compromised.

3. NOISY IMAGE

The Gaussian noise in digital images arise during acquisition eg. Sensor noise caused by poor illumination and or high temperature, and or transmission eg. Electronic circuit noise. The standard model of this noise is additive, independent at each pixel and independent of the signal intensity, caused primarily by Johnson–Nyquist noise such as thermal noise, including that which comes from the reset noise of capacitors such as kTC noise .Amplifier noise is a major part of the read noise of an image sensor, that is, of the constant noise level in dark areas of the image.

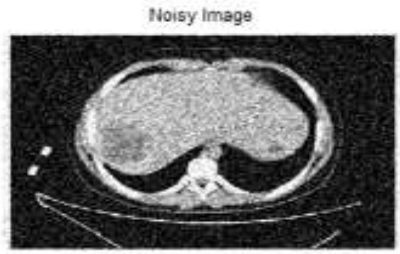

4. WIENER FILTER

The Wiener filter is a filter used to produce an estimate of a desired or target random process by linear time-invariant filtering an observed noisy process, assuming known stationary signal and noise spectra, and additive

noise. The Wiener filter minimizes the mean square error between the estimated random process and the desired process.

The goal of the Wiener filter is to filter out noise that has corrupted a signal. It is based on a statistical approach, and a more statistical account of the theory is given in the MMSE estimator article.

Typical filters are designed for a desired frequency response. However, the design of the Wiener filter takes a different approach. One is assumed to have knowledge of the spectral properties of the original signal and the noise, and one seeks the linear time-invariant filter whose output would come as close to the original signal as possible.

Wiener filters are characterized by the following:

- Assumption: signal and (additive) noise are stationary linear stochastic processes with known spectral characteristics or known autocorrelation and cross-correlation
- Requirement: the filter must be physically realizable/causal (this requirement can be dropped, resulting in a non-causal solution)
- Performance criterion: minimum mean-square error (MMSE)

Wiener Filter

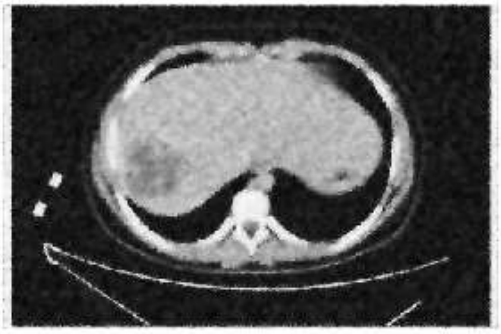

5. M-ASM SEGMENTATION

The active shape model (ASM) was inspired by deformable models with the added intention of limiting the extent of the model deformation. A statistical representation of an object is formed by identifying a set of landmark points on an object boundary and analyzing the variation of each across a set of training images. The ASM is then used to identify objects of the same class within other images. Deformation occurs as with deformable models but is restricted to within the bounds of the statistical model.

6. NODULE ENHANCEMENT

The CT Scans, CXRs and their equivalent dual-energy bone images in a training set for training the multi-resolution MTANN. One of the compensation of the MTANN technique is that it only desires a few number of dual-energy training images. In these cases, one was a normal case and the other three contained with nodules. The training samples for the nodules were extracted by manual in order to make it cover the nodule. The size of the sub-region for MTANNs was 9 × 9 pixels. It was adequate to cover the width of rib in the resolution image. Three-layered MTANNs were used in the experiments where the numbers of input, hidden, and output units were 81, 20, and 1, respectively. Fig. 4 shows the VDE bone image and the VDE soft tissue images with difference rib contrast processed by multi-resolution MTANN technique.

7. FEATURE EXTRACTION

Feature extraction involves simplifying the amount of resources required to describe a large set of data accurately. When performing analysis of complex data one of the major problems stems from the number of variables involved. Analysis with a large number of variables generally requires a large amount of memory and computation power or a classification algorithm which over fits the training sample and generalizes poorly to new samples. Feature extraction is a general term for methods of constructing combinations of the variables to get around these problems while still describing the data with sufficient accuracy.

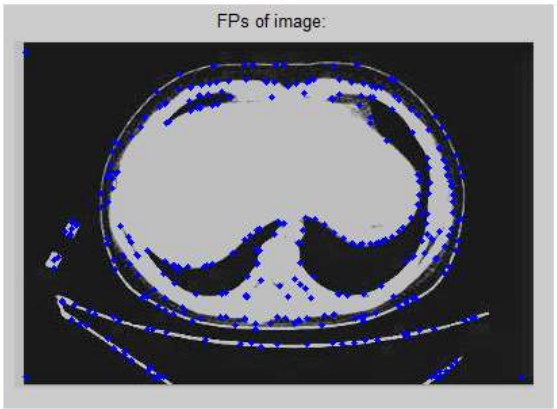

8. NODULE DETECTION WITH VDE

The Virtual Dual Energy is the image processing technique used to suppress the rib and clavicle. The Massive Training Artificial Neural Network is adequately trained with a small number of cases to demonstrate the distinction between nodules and vessels in thoracic Computed Tomography images. A lung nodule is clear as a spot on the lung that is 3 cm that is about 1 ½ inches in diameter or less. If an deviation is seen on an CT Scan of the lungs that is larger than 3 cm, it is considered a lung mass in its place of a nodule, and is more likely to be cancerous. Lung nodules usually need to be at least 1 cm in size before they can be seen on CT scan. Mean Square Error method is used to detect the nodule. The precision value, recall value, Fscore value is calculated. Precision value-relevant feature points Recall value-Exact feature point .Fscore value Calculated based on both precision and recall value.

9. STOCHASTIC WATERSHED SEGMENTATION

Stochastic watershed transformation is the mathematical morphology technique which improves the standard watershed algorithms when the aim is to segment complex images into a few regions. It is done by calculating the watershed regions for each nodules .And then find intensity values for watershed regions. Based on intensity values, classify the nodules.

Steps in stochastic watershed segmentation

- Calculating the gradient magnitude
- Watershed transform of gradient magnitude
- Opening
- Opening by reconstruction
- Opening-closing
- Opening-closing by reconstruction
- Regional maxima of Opening-closing by reconstruction
- Regional maxima superimposed on original image
- Modified Regional maxima superimposed on original image
- Threshold Opening-closing by reconstruction

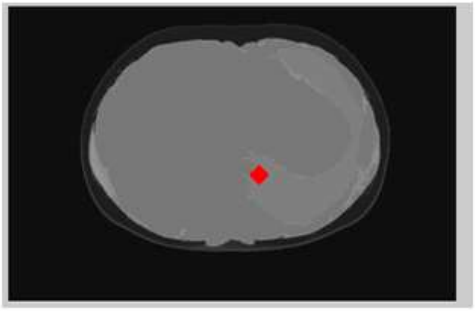

10. PERFORMANCE EVALUATION

The VDE-based CADe scheme achieved a sensitivity of 85.0%.The VDE-based CADe scheme not only can detect more nodules which were overlapped with ribs or clavicles, but also can reduce the FPs deduced by the ribs and clavicle. The VDE with Neural network classifier improves the sensitivity and it reduce the false positives than the SVM Classifier. The Morphology technique improves more sensitivity and reduce false positives.

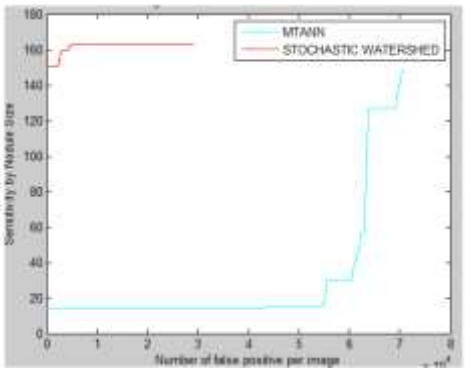

10. CONCLUSION

The segmentation technique is defined to detect the lung nodules. In addition an efficient Watershed algorithm is proposed for segmenting the lung nodule. Our experimental evaluation demonstrates that the stochastic watershed algorithm improves the sensitivity and reduced false positives when compared to all other segmentation techniques. our algorithm is good and scalable in detecting the lung nodules.

11. REFERENCES

1. Medical Image Segmentation: Methods and Software D.J. Withey and Z.J. Koles[1, 2] [1]Department of Electrical and Computer Engineering, [2]Department of Biomedical Engineering,University of Alberta, Edmonton, Alberta, CANADA T.F. Cootes, C.J. Taylor, D.H. Cooper, J. Graham, "Active shape models – Their training and application," *Comput. Vis. Image Understanding*, vol. 61,no. 1, pp. 38-59, 1995.

2. American Cancer Society, American Cancer Society Complete Guide to Complementary & Alternative Cancer Therapies, 2nd ed. Atlanta, GA.: American Cancer Society, 2009.

3. C. I. Henschke, D. I. McCauley, D. F. Yankelevitz, D. P. Naidich, G. McGuinness, O. S. Miettinen, D. M. Libby, M. W. Pasmantier, J. Koizumi, N. K. Altorki, and J. P. Smith, "Early lung cancer action project: Overall design and findings from baseline screening," Lancet, vol. 354, pp. 99–105, Jul. 10, 1999.

4. G. P. Murphy, W. Lawrence, R. E. Lenhard, and American Cancer Society, American Cancer Society Textbook of Clinical Oncology, 2nd ed. Atlanta, GA.: American Cancer Society, 1995.

5. H. Zhao, S. C. Lo, M. Freedman, and Y. Wang, "Enhanced lung cancer detection in temporal subtraction chest radiography using directional edge filtering techniques," presented at the Proc. SPIEMed. Imag.: Image Process., San Diego, CA, 2002.

6. J. H. Austin, B. M. Romney, and L. S. Goldsmith, "Missed bronchogenic carcinoma: Radiographic findings in 27 patients with a potentially resectable lesion evident in retrospect," Radiology, vol. 182, pp. 115–122, Jan. 1992.

7. P. K. Shah, J. H. Austin, C. S. White, P. Patel, L. B. Haramati, G. D. Pearson, M. C. Shiau, and Y. M. Berkmen, "Missed non-small cell lung cancer: Radiographic findings of potentially resectable lesions evident only in retrospect," Radiology, vol. 226, pp. 235–241, Jan. 2003.

8. F. Li, R. Engelmann, K. Doi, and H. MacMahon, "Improved detection of small lung cancers with dual-energy subtraction chest radiography," AJR Amer. J Roentgenol., vol. 190, pp. 886–891, Apr. 2008.

9. M. L. Giger, K. Doi, and H. MacMahon, "Image feature analysis and computer-aided diagnosis in digital radiography. 3. Automated detection of nodules in peripheral lung fields," Med. Phys., vol. 15, pp. 158–166, Mar.–Apr. 1988.

10. B. van Ginneken, B. M. ter Haar Romeny, and M. A. Viergever, "Computer-aided diagnosis in chest radiography: A survey," IEEE Trans. Med. Imag., vol. 20, no. 12, pp. 1228–1241, Dec. 2001.

11. T. Matsumoto, K. Doi, A. Kano, H. Nakamura, and T. Nakanishi, "Evaluation of the potential benefit of computer-aided diagnosis (CAD) for lung cancer screenings using photofluorography: Analysis of an observer study," Nippon Igaku Hoshasen Gakkai Zasshi, vol. 53, pp. 1195–1207, Oct. 25, 1993

12. Xin Sun Xiaoxiao Wang 'Study of edge detection algorithms for lung CT image on the basis of MATLAB' Control and Decision Conference (CCDC), 2011 Chinese ,2011

13. Dehmeshki, J. Amin, D. ; Valdivieso, M. ; Xujiong Ye 'Segmentation of Pulmonary Nodules in Thoracic CT Scans: A Region Growing Approach' Medical Imaging, IEEE Transactions on (Volume:27 , Issue: 4) April 2008

14. Samuel, C.C. ; Saravanan, V. ; Vimala Devi, M.R. 'Lung Nodule Diagnosis from CT Images Using Fuzzy Logic' International Conference on (Volume:3)2007

15. Sheng Chen and Suzuki, K 'Computerized Detection of Lung Nodules by Means of Virtual Dual Energy Radiography' IEEE Trans.vol.60,issue 2, pp .369 - 378 .Feb. 2013.